

The Strange Case of the Ethane Radical Cation†

Horst M. Sulzbach, Debrah Graham, Jeffrey C. Stephens and Henry F. Schaefer III*

Center for Computational Quantum Chemistry, The University of Georgia, Athens, Georgia 30602-2556 USA

Sulzbach, H. M., Graham, D., Stephens, J. C. and Schaefer, H. F. III, 1997. The Strange Case of the Ethane Radical Cation. – Acta Chem. Scand. 51: 547–555. © Acta Chemica Scandinavica 1997.

Energetically low-lying structures on the ethane radical cation potential energy surface are compared with the CCSD/DZP, BD/DZP, CCSD(T)/DZP, BD(T)/DZP, CCSD(T)/TZ2P, and CCSD(T)/TZ(2df,2pd)//CCSD(T)/TZ2P methods, and a number of density functional levels as well as second-order perturbation theory. The 2A_g state (C_{2h} symmetry) is only 0.28 kcal mol $^{-1}$ lower than the 2A_g state (D_{3d} symmetry) at BD(T)/DZP and 0.30 kcal mol $^{-1}$ at CCSD(T)/TZ(2df,2pd)//CCSD(T)/TZ2P. The two states are separated by a transition state which is less than 0.2 kcal mol $^{-1}$ above the energetically higher state, and inclusion of the ZPVE correction can reverse the ordering. The Born–Oppenheimer approximation is therefore not strictly valid and only one thermally averaged C_{2h} structure should be observed. A third $C_2H_6^+$ equilibrium geometry is obtained by removal of an electron from the second component of the e_g orbital of ethane (D_{3d} symmetry). It corresponds to either a 2B_g state (C_{2h} symmetry) or a ${}^2A''$ state (C_s symmetry), depending on whether the SOMO is spread out over both carbons or localized on one carbon only. This third minimum lies 3.37 kcal mol $^{-1}$ higher in energy than the 2A_g state at CCSD(T)/TZ(2df,2pd)//CCSD(T)/TZ2P. The ground state $C_2H_6^+$ barrier for rotation around the CC bond is estimated to be at least 1.0 kcal mol $^{-1}$, in disagreement with the experimental value of only 0.25 kcal mol $^{-1}$.

Most organic radical cations are formed by the loss of an electron from unsaturated or heteroatom-containing molecules so that the unpaired electron occupies the highest molecular π orbital or the non-bonding highest orbital of the heteroatom(s) with a π nature. In contrast with these cations the unpaired electron of alkane cations is expected to occupy the highest σ bonding orbital. For most saturated hydrocarbons the determination of this highest σ bonding orbital is straightforward, but in the case of the ethane radical cation, several different orbitals have to be taken into account. The electronic configuration of ground state, neutral ethane (D_{3d} symmetry) is known to be $(1a_{1g})^2(1a_{2u})^2(2a_{1g})^2(2a_{2u})^2(1e_u)^4(3a_{1g})^2(1e_g)^4$. According to Koopmans' theorem¹ the electron removal with the smallest ionization potential should occur from the $1e_g$ orbital. Since the 2E_g state of $C_2H_6^+$ is doubly degenerate in the D_{3d} equilibrium geometry of the neutral molecule, Jahn–Teller distortion^{2–4} of the resulting radical cation should lower the molecular symmetry to C_{2h} and give rise to either a 2B_g or a 2A_g state, depending on which of the two formerly degenerate orbitals is the singly occupied molecular orbital (SOMO) (compare Fig. 1). Furthermore, since both $1e_g$ orbitals

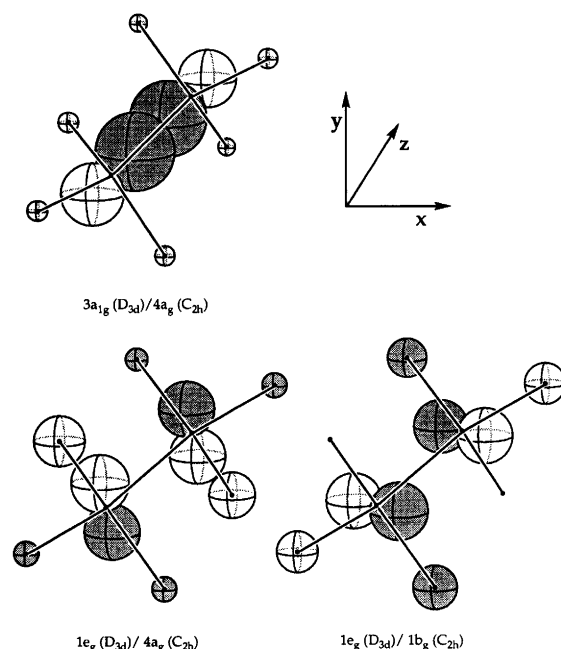


Fig. 1. Orientation and shape of the $3a_{1g}$ orbital (top) and the $1e_g$ orbitals of neutral ethane (bottom). If the symmetry is lowered to C_{2h} with the yz plane as the remaining plane of symmetry (second column), both the $3a_{1g}$ and the first $1e_g$ orbital transform as A_g .

* To whom correspondence should be addressed.

† Lecture held at the 14th International Conference on Radical Ions, Uppsala, Sweden, July 1–5, 1996.

(D_{3d} symmetry) are weakly antibonding across the CC bond, the ethane radical cation should possess a shorter CC bond than neutral ethane.

However, the first *ab initio* analysis of the ethane radical cation led to a ${}^2A_{1g}$ state (D_{3d} symmetry) with a CC bond length of about 1.9 Å as the absolute minimum.^{5,6} This ${}^2A_{1g}$ state corresponds to a $C_2H_6^+$ molecule in which the electron has been removed from the second highest molecular orbital ($3a_{1g}$) instead from the HOMO. The minimum that corresponds to the 2B_g component (C_{2h} symmetry) of the former 2E_g state (D_{3d} symmetry) was also located, but at the UHF/4-31G//UHF/STO-3G level it was almost 26 kcal mol⁻¹ higher in energy than the ${}^2A_{1g}$ structure.^{5,6} No minimum was found for the 2A_g component (C_{2h} symmetry) of the former 2E_g state (D_{3d} symmetry) at the UHF level of theory.

The photoelectron spectrum of $C_2H_6^+$, which shows low energy peaks at 12.0 eV, 12.7 eV, and 13.4 eV, is difficult to interpret. Most experimentalists believe that the irregular vibrational progression, with its numerous shoulders and small peaks observed below 12.55 eV, strongly suggests that vibronic interaction is occurring in this transition. Manifestations such as this, i.e., Jahn–Teller interactions,³ occur when degenerate vibrational modes are excited in a degenerate electronic state. Consequently, the 12.00 eV and 12.72 eV peaks are assigned to the transitions that occur from the $1e_g$ orbitals, and the peak at 13.4 eV is thought to be due to removal of an electron from the $3a_{1g}$ orbital.^{2,7,8} This assignment is consistent with the energetic ordering of the orbitals in neutral ethane.

Most of the complexity that is encountered when the 2A_g state (C_{2h} symmetry) of the ethane radical cation is studied arises from the fact that Jahn–Teller distortion³ has lowered the molecular symmetry from D_{3d} to C_{2h} , and both the former $3a_{1g}$ orbital and one of the two formerly degenerate e_g orbitals now belong to the irreducible representation that transforms as A_g (compare Fig. 1). Consequently, as discussed in detail by Richartz *et al.*,^{9,10} any minimum on the 2A_g potential energy surface is an optimal mixture of 2E_g and ${}^2A_{1g}$ character. At short CC distances the former is more important, while for larger CC bond lengths the ${}^2A_{1g}$ contribution dominates. The observed ${}^2A_{1g}$ minimum with the long CC bond is a pure ${}^2A_{1g}$ state (D_{3d} symmetry). Any structure with a shorter CC bond length will contain contributions of both the $a_g(3a_{1g})$ and the $a_g(1e_g)$ orbitals.¹¹ This mixing of the two a_g orbitals in the C_{2h} point group also leads to an extremely flat potential energy surface for the CC stretch.⁹ Since the $a_g(a_{1g})$ orbital (C_{2h} symmetry) is strongly bonding across the CC bond, the fact that it becomes the SOMO instead of the $a_g(e_g)$ orbital at large CC distances is not unexpected. It does not violate Koopmans' theorem because the change in the SOMO is accompanied by a large geometrical reorganization of the molecule.

That the ${}^2A_{1g}$ state is the absolute minimum on the

potential energy hypersurface of the ethane radical cation, as predicted by MNDO and early *ab initio* results, is questioned by electron spin resonance (ESR) experiments.^{12–15} At 4.2 K a 1:2:1 triplet with a hyperfine coupling constant of 153 G is observed. This splitting pattern is only consistent with a 2A_g state with C_{2h} symmetry and a diborane-like structure. The electron is removed from the a_g orbital that is strongly CH bonding along the CH bonds that are in the plane of the molecule and would have negligible coefficients at the other four hydrogen atoms (Fig. 1). The ${}^2A_{1g}$ state should give a septet with a much smaller coupling constant, because the $3a_{1g}$ orbital is mainly CC bonding and has only small coefficients at the hydrogen atoms (compare Fig. 1). The 2B_g state should give rise to a quintet due to the four equivalent hydrogen atoms with large MO coefficients (compare Fig. 1) in the b_g orbital. Hence, ESR experiments deduce a 2A_g state which consists mainly of the $a_g(e_g)$ orbital with a CC bond length near that of neutral ethane, and only a small contribution of the $a_g(a_{1g})$ orbital.

Lunell and Huang were the first to predict the existence of this 2A_g minimum at MP2/6-31G**.¹⁶ At this level the diborane-like 2A_g minimum with a HCC bond angle of the bridging hydrogens of only 83° is 0.35 kcal mol⁻¹ lower in energy than the ${}^2A_{1g}$ structure with the long CC bond.¹⁷ Consecutive studies showed that this structure remains a stationary point at MP2 for all basis sets of equal or larger size.¹⁷ In addition, the ESR parameters that are theoretically derived for the 2A_g minimum are in reasonable agreement with the experimental data.^{16–19} Eriksson *et al.* were also able to locate the short bond 2A_g minimum with density functional methods, but no energetic ordering is given.¹⁹

In this paper the results and discussion section consists of two parts. In the first CCSD, CCSD(T), BD and BD(T)²⁰ are employed to obtain reliable structures and energies for the 2B_g , 2A_g and the ${}^2A_{1g}$ states of $C_2H_6^+$. These data are compared with each other, with the values that are obtained with second-order Møller–Plesset perturbation theory (MP2), and with the results of various standard density functional methods. In addition, a structure of the 2A_g state of $C_2H_6^+$ is optimized for each 0.1 Å interval between 1.5 Å and 2.0 Å at the CCSD level of theory. The corresponding ROHF molecular orbitals that are obtained for these geometries are used for a detailed discussion of the mixing between the 2A_g and the ${}^2A_{1g}$ states. In the second part of the discussion section the barrier for going from the 2A_g minimum to the ${}^2A_{1g}$ minimum, as well as the barrier for rotation around the CC bond, is determined and compared with literature data where available. Dynamic ESR measurements of partially deuterated ethane radical cations yield a barrier for the rotation around the CC bond of about 0.25 kcal mol⁻¹.¹⁵ Earlier studies at the MP4 level by Eriksson and Lunell give a barrier of 1.1 kcal mol⁻¹ for this rotation.²¹ The corresponding transition state (C_{2v} symmetry) has a CC bond length of 1.97 Å. We were

further interested to see whether this transition state connected two 2A_g minima directly, as assumed by Eriksson and Lunell, or rather two ${}^2A_{1g}$ structures.

Methods and computational details

All structures in this study were fully optimized if not specified otherwise. Geometry optimizations that employed second-order Møller–Plesset perturbation theory or density functional theory (DFT) methods were carried out with the GAUSSIAN 94 package.²² The DFT study employed three different combinations of functionals: BLYP, Becke3LYP and BHandHLYP. BLYP is a pure DFT method in which the Hartree–Fock (HF) exchange integral has been substituted with Becke’s 1988 exchange functional (B),²³ and which employs the gradient corrected correlation functional of Lee–Yang and Parr (LYP).^{24,25} Becke3 and BHandH are both hybrid functionals in which the exact term for the HF exchange integral has been replaced by a mixture of the HF exchange and a DFT functional. Becke3 designates Becke’s three-parameter functional,^{26,27} while BHandH, which was first introduced in GAUSSIAN92/DFT, is similar to Becke’s ‘half and half’ functional.²⁷ In combination with the LYP correlation functional the hybrid methods Becke3LYP and BHandHLYP are obtained. The ACES II program system²⁸ was used to optimize the geometries at the CCSD [coupled cluster (CC) with single (S) and double (D) excitations] and CCSD(T) (CCSD with additional inclusion of perturbative triple excitations) levels. Analytic gradient methods were employed for the CCSD and CCSD(T) optimizations.

Davidson and Borden have pointed out in general that if the form assumed for the wavefunction is oversimplified, as is often the case for wavefunctions that consist of a single Slater determinant, broken symmetry solutions may be obtained as minima from energy optimizations.²⁹ If the optimized wavefunction does not transform as any irreducible representation of the point group of the molecule, application of the symmetry operators will generate related wavefunctions. The energy will then show an artifactual cusp for the structure of high symmetry, and broken symmetry structures may appear as minima on a calculated potential energy surface.²⁹ Since at the very highest levels of theory second derivatives can only be obtained by finite displacement methods, artificial symmetry breaking makes the determination of the second derivatives impossible. To avoid this problem we also employed Brueckner orbitals^{30–34} in the present studies of $C_2H_6^+$ at the coupled-cluster level. The resulting methods are named BD if all double excitations are included, and BD(T) if in addition to all double excitations connected perturbative triples are included. In the B–CC method the Brueckner orbitals correspond to the cluster expansion for which ($T_1 = 0$). The merits of Brueckner orbitals are that the bulk of the orbital adjustment required by the correlated wavefunction has been accounted for, and, as a result, the wavefunction

should be much less susceptible to artificial symmetry breaking. The BD and BD(T) calculations were also performed with the ACES II program system, but the energy gradients had to be obtained by finite displacement methods, since analytic gradients are not available for those methods.

The Huzinaga double zeta (DZ) C(9s5p/4s2p), H(4s/2s) basis set³⁵ in Dunning’s contraction³⁶ augmented with a set of six Cartesian d polarization functions on carbon (orbital exponent $\alpha_d = 0.654$) and a set of three p polarization functions on hydrogen (orbital exponent $\alpha_p = 0.70$) was employed.³⁷ This DZP basis set was used in all calculations that are not mentioned otherwise. In addition, all geometries were also optimized at CCSD(T) for a triple zeta C(10s6p/5s3p), H(5s3p/3s2p) Huzinaga basis set³⁵ in Dunning’s contraction³⁸ augmented with two sets of six Cartesian d polarization functions (3d/2d) on carbon and two sets of three p polarization functions on hydrogen (3p/2p), namely TZ2P. To investigate the effect of a further increase in the basis set, energy single points for the structures optimized at CCSD(T)/TZ2P were computed for a triple-zeta C(10s6p/5s3p), H(5s/3s) Huzinaga basis-set³⁵ in Dunning’s contraction³⁸ augmented with two sets of six Cartesian d polarization functions (orbital exponents $\alpha_{d1} = 1.50$ and $\alpha_{d2} = 0.375$) and one set of ten Cartesian f functions (orbital exponent $\alpha_f = 0.8$) on carbon and two sets of p polarization functions (orbital exponents $\alpha_{p1} = 1.50$ and $\alpha_{p2} = 0.375$) and one set of six Cartesian d functions (orbital exponent $\alpha_d = 1.0$) on hydrogen at the CCSD(T) level of theory with PSI.³⁹ The latter basis set is designated TZ(2df,2pd).

All computations were carried out on IBM 3CT RS-6000 workstations at the Center for Computational Quantum Chemistry, the University of Georgia, Athens, Georgia.

Results and discussion

Geometries. The geometrical details for all structures are given in Figs. 2 to 5. The D_{3d} minimum that corresponds to the ${}^2A_{1g}$ state (Fig. 2) has a CC bond distance somewhat longer than 1.9 Å. The CH_3 groups are almost planar with an HCC bond angle of only 98°. The geometry of this state does not depend strongly on the level of theory and our results are in good agreement with those of previous studies.^{5,6,17,18,40,41}

The 2A_g state (C_{2h} symmetry) yields a diborane-like structure (Fig. 3). The bond angle between the CH bond that lies in the molecular symmetry plane, and the CC bond is only about 82° and the corresponding CH bond length is significantly elongated (Fig. 3). The geometry of this state is significantly affected by changes in the level of theory. While the SOMO in the D_{3d} structure is comprised only of the $3a_{1g}$ orbital that is also found in neutral ethane, the SOMO of the 2A_g state has contributions from both the $3a_{1g}$ orbital of ethane and the $1e_g$ orbital of ethane, which has its p-AOs oriented along

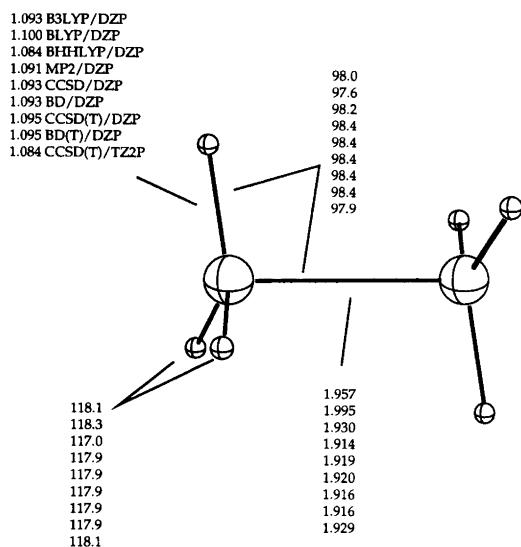


Fig. 2. Geometrical details for the ${}^2A_{1g}$ minimum (D_{3d} symmetry) at the Becke3LYP/DZP, BLYP/DZP, BHandHLYP/DZP, MP2/DZP, CCSD/DZP, BD/DZP, CCSD(T)/DZP, BD(T)/DZP, and CCSD(T)/TZ2P levels of theory. All bond lengths are in Å and all angles in degrees.

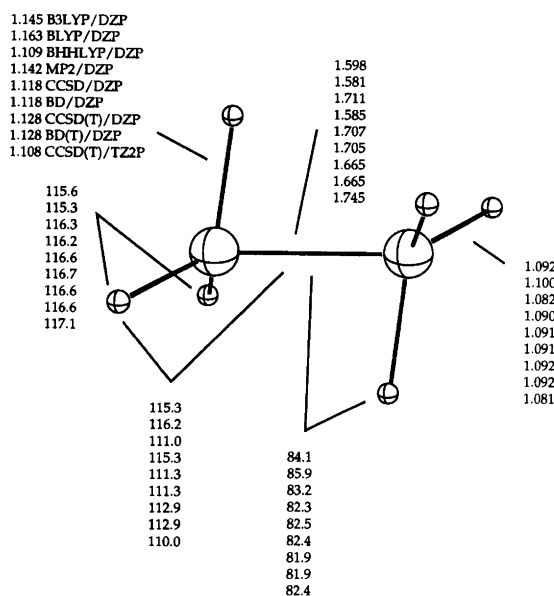


Fig. 3. Geometrical details for the 2A_g minimum (C_{2h} symmetry) at the Becke3LYP/DZP, BLYP/DZP, BHandHLYP/DZP, MP2/DZP, CCSD/DZP, BD/DZP, CCSD(T)/DZP, BD(T)/DZP, and CCSD(T)/TZ2P levels of theory. All bond lengths are in Å and all angles in degrees.

the y -axis (compare Fig. 1). Both of these MOs transform as A_g in the C_{2h} point group and mix to form two new a_g orbitals. The energetically lower lying one is doubly occupied and the unfavorable combination becomes the SOMO. Since this high-lying orbital is only singly occupied, the net result is a lowering of the energy. Fig. 6 shows how the contributions of the $a_g(1e_g)$ and the $a_g(3a_{1g})$ orbitals to the SOMO change as a function of the CC bond length. The optimal mixture will depend

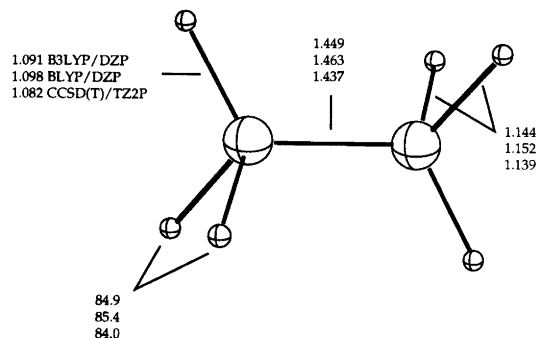


Fig. 4. Geometrical details for the 2B_g structure (C_{2h} symmetry) at all levels where it corresponds to a minimum [Becke3LYP/DZP, BLYP/DZP, and CCSD(T)/TZ2P]. All bond lengths are in Å and all angles in degrees.

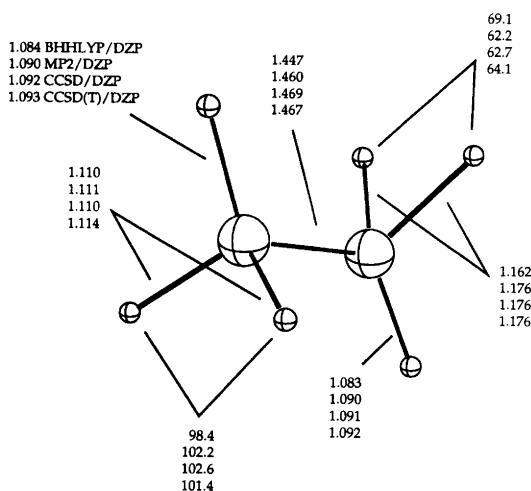


Fig. 5. Geometrical details for the ${}^2A''$ structure (C_s symmetry) at all levels where it corresponds to a minimum [BHandHLYP/DZP, MP2/DZP, CCSD/DZP, and CCSD(T)/DZP]. All bond lengths are in Å and all angles in degrees.

strongly on the relative orbital energy of the mixing $1e_g$ and $3a_{1g}$ orbitals. The hypothetical 2A_g state with a SOMO which would consist entirely of the former $1e_g$ orbital should have a CC bond length of about 1.45 Å (compare Figs. 4 and 5), while the D_{3d} minimum has a CC bond length of about 1.9 Å. Even if the ratio of the $a_g(1e_g)$ to the $a_g(3a_{1g})$ contribution changes only slightly, changes in the CC bond length of more than 0.1 Å will be the consequence. Hence, while the CC bond length is 1.67 Å at CCSD(T)/DZP, it increases to 1.75 Å if the TZ2P basis set is employed instead of the DZP basis set. Similarly, the CC bond lengths that are predicted by the DFT methods differ by 0.13 Å (Fig. 3). However, all methods agree that the structure is clearly diborane-like with an HCC angle of only 82–84°. ⁴²

Removal of an electron from the second component of the $1e_g$ orbital leads to the third energetically low lying state. Previous studies report that it has C_{2h} symmetry and that the corresponding electronic state is 2B_g .^{5,6} We find that this is only true at the CCSD(T)/TZ2P, Becke3LYP/DZP, and BLYP/DZP

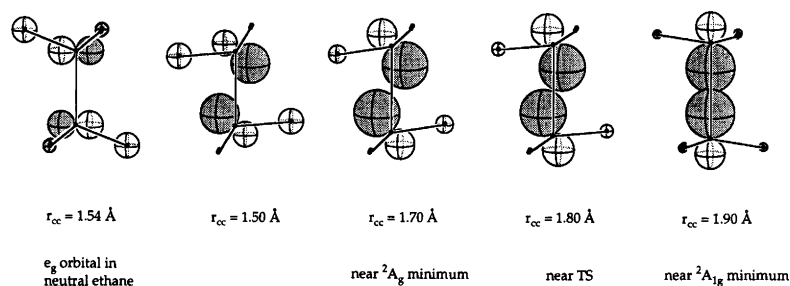


Fig. 6. Change in the MO contributions to the SOMO of the 2A_g state of $C_2H_6^+$ as a function of the CC bond length. Given below the CC bond length is the structure that corresponds to that CC distance.

levels of theory (Fig. 4). At all other levels this minimum has only C_s symmetry and the corresponding electronic state is ${}^2A''$ (Fig. 5). Fig. 7 shows that the C_s structure is a consequence of a localization of the radical center on one of the two CH_3 groups. The components of the $1e_u$ and $1e_g$ orbitals with a node in the yz plane are now each localized on one of the two carbon centers instead of on both. As a consequence the HCH angles between the pairs of symmetry-equivalent hydrogens on the two sides of the molecules are very different. The HCH angle on the side where the SOMO is located is only about 65° , while the other one is about 100° . Both are about 85° for the 2B_g state (Fig. 5).

Energies. Table 1 lists the absolute energies of the three energetically lowest lying states of $C_2H_6^+$ at various levels. Table 2 compares their relative energies. At MP2 the 2A_g state (CC distance 1.585 Å) is lowest in energy, followed by the ${}^2A_{1g}$ state (CC distance 1.914 Å) which lies 1.6 kcal mol $^{-1}$ above the latter. Our MP2 results employed a DZP basis set, while those of Lunell and

Huang, who find the 2A_g state to be only 0.35 kcal mol $^{-1}$ more stable, were obtained for a 6-31G** basis set.¹⁶ This might account for the disagreement. However, it is rather surprising that a very small improvement in the basis set has such a pronounced effect on the energy gap between the 2A_g and the ${}^2A_{1g}$ states.

The CCSD/DZP and BD/DZP methods find the ${}^2A_{1g}$ state to be lower than the 2A_g state, but the energy gap between the two states is now only about 0.3 kcal mol $^{-1}$. Inclusion of the ZPVE correction increases the gap slightly to 0.7 kcal mol $^{-1}$. Unlike CCSD, the BD method should be largely unaffected by artificial symmetry breaking. The excellent agreement between CCSD and BD [and also between CCSD(T) and BD(T), compare Table 2] demonstrates that artificial symmetry breaking does not occur for $C_2H_6^+$. Furthermore, the fact that the T_1 amplitudes of all structures in this study are smaller than 0.02 justifies a single reference treatment. The inclusion of perturbative triple excitations lowers the energy of the 2A_g state slightly more than that of the ${}^2A_{1g}$ state. At CCSD(T)/DZP and BD(T)/DZP the 2A_g state is 0.7 kcal mol $^{-1}$ more stable than the ${}^2A_{1g}$ state. However, inclusion of the ZPVE correction reduces the difference to a mere 0.3 kcal mol $^{-1}$. At CCSD(T)/TZ2P the energetic ordering is reversed once more and after ZPVE correction the ${}^2A_{1g}$ state is 0.4 kcal mol $^{-1}$ more stable. To investigate the effect of an even larger basis set on the energy difference between the 2A_g and the ${}^2A_{1g}$ states, we appended a TZ2P basis set with a set of f functions on carbon and d functions on hydrogen to obtain single-point energies based on the CCSD(T)/TZ2P geometry. At this computationally intensive CCSD(T)/TZ(2df,2pd)//CCSD(T)/TZ2P level the trend is reversed and the 2A_g state is 0.43 kcal mol $^{-1}$ lower in energy than the ${}^2A_{1g}$ state (0.30 kcal mol $^{-1}$ after correction for the ZPVE).

Finally, the third low-lying $C_2H_6^+$ structure, regardless of whether it is a 2B_g state (C_{2h} symmetry) or a ${}^2A''$ state (C_s symmetry), is about 3–5 kcal mol $^{-1}$ higher in energy than the 2A_g and the ${}^2A_{1g}$ state at all correlated *ab initio* methods.

In contrast with the coupled-cluster methods, the results of the density functional methods depend strongly on the functional employed. Becke3LYP and BLYP

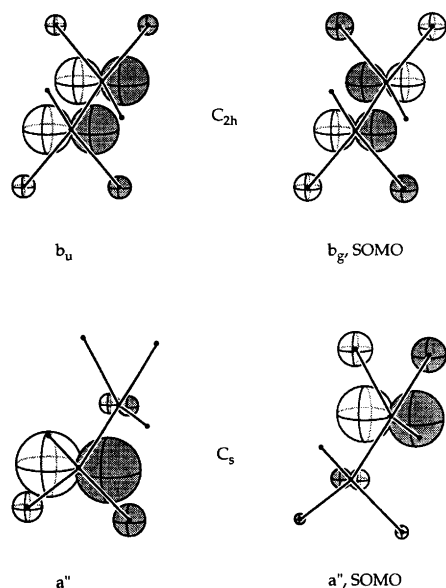


Fig. 7. Comparison of the two energetically highest π -type orbitals of the 2B_g (C_{2h}) and ${}^2A''$ (C_s) states.

Table 1. Absolute energies (Hartree) of the three energetically lowest lying structures of $C_2H_6^+$ at Becke3LYP, BLYP, BHandHLYP, MP2, CCSD, BD, CCSD(T), BD(T), CCSD(T)/TZ2P, and CCSD(T)/TZ(2df,2pd)//CCSD(T)/TZ2P. Where no basis-set is explicitly specified, a Huzinaga double zeta basis in Dunning's contraction with added polarization functions on both hydrogen and carbon (DZP) was employed. Given in parentheses is the molecular orbital of ethane from which the electron was removed to arrive at the respective cation state.

	2B_g (C_{2h}) or ${}^2A''$ state (C_s) (e_g orbital containing p_x^a)		2A_g state (C_{2h} symmetry) (e_g orbital containing p_y^a).	${}^2A_{1g}$ state (D_{3d} symmetry) (a_{1g} orbital ^a). Abs. energy
	Symmetry	Abs. energy	Abs. energy	
MP2 ^b	C_s	-79.14690	-79.15500	-79.15242
Becke3LYP	C_{2h}	-79.42353	-79.42562	-79.42280
BLYP	C_{2h}	-79.37050	-79.36900	-79.36474
BHandHLYP	C_s	-79.35726	-79.36582	-79.36656
CCSD	C_s	-79.18891	-79.19878	-79.19924
BD	^c		-79.19855	-79.19913
CCSD(T)	C_s	-79.19775	-79.20692	-79.20588
BD(T)	^c		-79.20693	-79.20589
CCSD(T)/TZ2P	C_{2h}	-79.24812	-79.25940	-79.25978
CCSD(T)/TZ(2df,2pd)				
//CCSD(T)/TZ2P	C_{2h}	-79.28238	-79.29192	-79.29123

^aFor a visualization of the orbitals compare Fig. 1. ^bTo be consistent with the CC methods, all electrons were correlated (MP2 = Full). ^cSize limitations in the ACESII program package did not allow the computation of $C_2H_6^+$ in C_s symmetry.

Table 2. Relative energies (kcal mol⁻¹) of the three energetically lowest lying structures of $C_2H_6^+$ at Becke3LYP, BLYP, BHandHLYP, MP2, CCSD, BD, CCSD(T), BD(T), CCSD(T)/TZ2P, and CCSD(T)/TZ(2df,2pd)//CCSD(T)/TZ2P. Where no basis set is explicitly specified, a Huzinaga double zeta basis in Dunning's contraction with added polarization functions on both hydrogen and carbon (DZP) was employed.

	2B_g (C_{2h}) or ${}^2A''$ state (C_s)		2A_g state (C_{2h} symmetry)		${}^2A_{1g}$ state (D_{3d} symmetry)	
	Rel. energy	With ZPVE	Rel. energy	With ZPVE	Rel. energy	With ZPVE
MP2	5.08	3.68	0.00	0.00	1.62	1.62
Becke3LYP	1.32	0.00	0.00	1.31	1.77	2.94
BLYP ^a	0.00	0.00	0.94	3.56	3.62	6.10
BHandHLYP	5.84	3.44	0.47	0.55	0.00	0.00
CCSD ^b	6.48	5.05	0.29	0.67	0.00	0.00
BD ^b			0.37	0.74	0.00	0.00
CCSD(T)	5.76	3.95	0.00	0.00	0.65	0.28
BD(T) ^b			0.00	0.00	0.65	0.28
CCSD(T)/TZ2P ^a	7.32	4.84	0.24	0.38	0.00	0.00
CCSD(T)/TZ(2df,2pd)	5.98	3.37	0.00	0.00	0.43	0.30
//CCSD(T)/TZ2P ^a						

^aBecke3LYP/DZP frequencies were employed for the ZPVE correction. ^bCCSD(T)/DZP frequencies were employed for the ZPVE correction.

predict the 2B_g state to be lowest in energy, closely followed by the 2A_g state. The ${}^2A_{1g}$ state is 2–6 kcal mol⁻¹ higher in energy at Becke3LYP and BLYP (Table 2). At BHandHLYP a much different energetic ordering of the three states is obtained. In agreement with the CCSD results, the ${}^2A_{1g}$ state is lowest in energy followed by the 2A_g state which is predicted to be only 0.5 kcal mol⁻¹ higher in energy. The second minimum that is obtained from the e_g orbital corresponds now to a ${}^2A''$ state (C_s symmetry) and is about 5 kcal mol⁻¹ higher in energy.

We conclude that at the highest levels of theory the ${}^2A_{1g}$ and the 2A_g states are nearly degenerate in energy and small changes in the computational method can lead to a reversal of the energetic ordering. The third low-lying structure corresponds to either a 2B_g (C_{2h} symmetry)

or a ${}^2A''$ state (C_s symmetry) and is about 3–5 kcal mol⁻¹ higher in energy. The huge difference between the Becke3LYP and BLYP results on the one hand and the BHandHLYP results on the other hand suggests further that density functional methods may not be suitable to study this problem. The failure of the DFT methods can be explained if we assume that the 2B_g state is affected more by correlation effects than the two other states, and that Becke3LYP and BLYP overestimate the extent of the electron correlation. However, such assumptions are highly speculative and our data are not sufficient to give a final answer.

Transition states. ESR experiments with ethane radical cations in which some of the hydrogens had been substituted by deuterium yield a barrier to rotation around

Table 3. Relative energies (kcal mol⁻¹) of the minimum of the ²A_{1g} state, the TS for the CC bond stretch, and the TS for CC bond rotation with respect to the ²A_g minimum of C₂H₆⁺ for the MP2, Becke3LYP, BLYP, BHandH, CCSD, CCSD(T), CCSD(T)/TZ2P, and CCSD(T)/TZ(2df,2pd)//CCSD(T)/TZ2P methods. Where no basis set is explicitly specified, a Huzinaga double zeta basis in Dunning's contraction with added polarization functions on both hydrogen and carbon (DZP) was employed.

	² A _g minimum		² A _{1g} minimum		TS for CC stretch		TS for CC bond rotation	
	Rel. energy	With ZPVE	Rel. energy	With ZPVE	Rel. energy	With ZPVE	Rel. energy	With ZPVE
MP2	0.00	0.00	1.62	1.62	1.80	1.64	3.44	3.00
B3LYP	0.00	0.00	1.77	1.63	1.79	1.61	3.27	2.62
BLYP ^a	0.00	0.00	2.68	2.54	2.68	2.49	4.02	3.37
BHandH	0.00	0.00	-0.47	-0.55	0.00	-0.13	1.16	0.69
CCSD ^b	0.00	0.00	-0.29	-0.67	0.08	-0.40	1.46	0.55
CCSD(T)	0.00	0.00	0.65	0.28	0.75	0.27	2.43	1.52
CCSD(T)/TZ2P ^a	0.00	0.00	-0.24	-0.38	0.02	-0.17	1.20	0.56
CCSD(T)/TZ(2df,2pd) //CCSD(T)/TZ2P ^a	0.00	0.00	0.43	0.30	^c		2.00	1.35

^aBecke3LYP/DZP frequencies were employed for the ZPVE correction. ^bCCSD(T)/DZP frequencies were employed for the ZPVE correction. ^cAn energy single point was not computed, because the energetic ordering of the ²A_g state and the ²A_{1g} state changes and hence a very different geometry for this TS is expected.

the CC bond of about 0.25 kcal mol⁻¹ for the unsubstituted radical cation and of about 0.5 kcal mol⁻¹ for the singly deuteriated isomer.¹⁵ Erikson and Lunell obtained a TS with C_{2v} symmetry and a barrier height of 1.1 kcal mol⁻¹ at MP4/6-31G** and of 2.2 kcal mol⁻¹ at MP2/6-31G**. ²¹ Our results for the transition state of rotation are summarized in Table 3. Fig. 8 summarizes the geometrical details of this TS at various levels of theory. Unlike Eriksson and Lunell we find that this TS has true D_{3h} symmetry rather than C_{2v} symmetry. Both the CC bond length and the HCC bond angle are very similar to those found for the ²A_{1g} minimum. An intrinsic reaction coordinate (IRC) following at the MP2/DZP level showed that this TS indeed connects two ²A_{1g} minima. A comparison of the barrier height with respect to the experimentally observed ²A_g minimum (Fig. 3) is

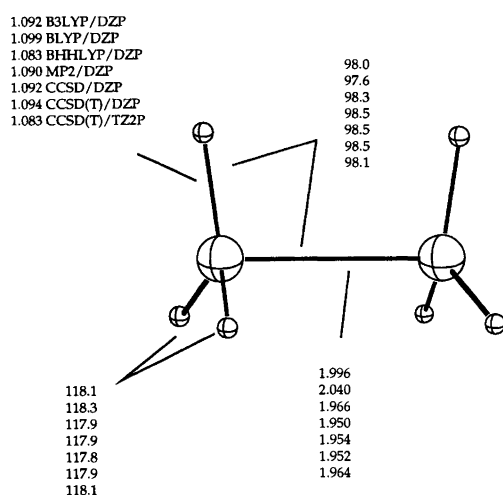


Fig. 8. Geometrical details for the TS of rotation (D_{3h} symmetry) at the Becke3LYP/DZP, BLYP/DZP, BHandHLYP/DZP, MP2/DZP, CCSD/DZP, CCSD(T)/DZP, and CCSD(T)/TZ2P levels of theory. All bond lengths are in Å and all angles in degrees.

given in Table 3. It shows that the barrier to rotation depends strongly on the level of theory. At our best level, CCSD(T)/TZ(2df,2pd)//CCSD(T)/TZ2P, the barrier with respect to the ²A_g state (Table 3) is computed to be 1.35 kcal mol⁻¹ after inclusion of the ZPVE correction. This value deviates by more than 1.0 kcal mol⁻¹ from the experimentally determined 0.25 kcal mol⁻¹. Most of the change in the barrier height is due to changes in the relative stability of the ²A_g minimum with respect to the ²A_{1g} minimum. If the relative energy of the TS for rotation with respect to the ²A_{1g} minimum is compared, the barrier is predicted to be between 0.8 and 1.4 kcal mol⁻¹ at all levels. This is physically more meaningful since the TS connects two ²A_{1g} minima.

As discussed above, the TS for rotation connects two ²A_{1g} minima. However, the ²A_g minimum is the experimentally observed structure. In order for a scrambling of the deuterium label(s) to occur, the ethane radical cation must first go from the ²A_g minimum to the ²A_{1g} minimum from which it can then rotate to change the position of the deuterium label. We were interested in the structure and energy of the TS that connects the ²A_g and the ²A_{1g} minima (Fig. 9) and which has not been characterized previously. Table 3 shows that this TS lies at most 0.1 kcal mol⁻¹ above the energetically less favorable minimum. Whether this minimum corresponds to the ²A_g or the ²A_{1g} state depends on the level of theory. This extremely low barrier is understood if one recalls the fact that the a_g(e_g) and the a_g(a_{1g}) orbitals mix to form the SOMO. This mixing leads to two minima: one in which the SOMO is a pure a_{1g} orbital and one where it has sizable contributions of both the a_g(e_g) and the a_g(a_{1g}) MOs. However, at all CC bond lengths a fairly favorable mixture of the two MOs is possible, and hence, even the TS is very low in energy. The small imaginary frequency of only about 200 cm⁻¹ that corresponds to the CC bond stretch further documents the ease with

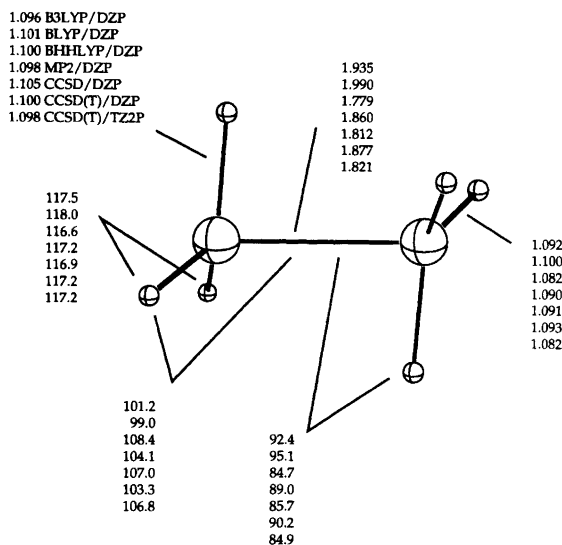


Fig. 9. Geometrical details for the TS (C_s symmetry) that connects the 2A_g and the ${}^2A_{1g}$ states at the Becke3LYP/DZP, BLYP/DZP, BHandHLYP/DZP, MP2/DZP, CCSD/DZP, CCSD(T)/DZP, and CCSD(T)/TZ2P levels of theory. All bond lengths are in Å and all angles in degrees.

which the CC bond length can be changed. This raises the question of whether an *ab initio* treatment based on the Born–Oppenheimer approximation is still appropriate to describe the 2A_g state and the ${}^2A_{1g}$ state of the ethane radical cation. Once the ZPVE correction has been applied to the energies, the TS for the bond stretch is lower than one of the minima at some of the best levels in our study. Schreiner *et al.* have observed a similar situation for the CH_5^+ cation.⁴³ We suggest that an *ab initio* approach which would allow a coupling between the motion of the nuclei that corresponds to the CC bond stretch and the motion of the electrons would yield only one averaged minimum with C_{2h} symmetry, instead of the 2A_g and the ${}^2A_{1g}$ minima. Since at our best level CCSD(T)/TZ(2df,2pd)//CCSD(T)/TZ2P the 2A_g state is lower in energy than the ${}^2A_{1g}$ state, the averaged minimum should resemble the diborane-like structure more than the D_{3d} structure. The ESR spectrum that would be obtained for such an averaged structure should therefore be in reasonable agreement with the experimental findings.

Conclusions

At very high levels of theory the 2A_g state (C_{2h} symmetry, CC distance ~ 1.7 Å) and the ${}^2A_{1g}$ state (D_{3d} symmetry, CC distance ~ 1.9 Å) of the ethane radical cation are nearly degenerate in energy. While the ${}^2A_{1g}$ state is obtained simply by removal of an electron from the $3a_{1g}$ orbital of neutral ethane, the SOMO of the 2A_g state is a mixture of both the $3a_{1g}$ and $1e_g$ orbitals of neutral ethane. The contribution of the $3a_{1g}$ orbital causes the 2A_g state to have a CC bond length intermediate in bond order between 1/2 and 1. Furthermore, the potential

energy surface is extremely flat with respect to a variation of the CC bond length, because an energetically favorable combination of the $3a_{1g}$ and $1e_g$ orbitals exists for any bond length between 1.5 Å and the 1.9 Å of the pure ${}^2A_{1g}$ minimum.

At CCSD(T)/TZ(2df,2pd)//CCSD(T)/TZ2P, the most elaborate level in this study, the 2A_g state is 0.30 kcal mol⁻¹ lower in energy than the ${}^2A_{1g}$ state after correction for the ZPVE. The transition state that separates these two minima is also very low in energy. As a consequence the ZPVE is large enough to equilibrate the two minima at all temperatures, and only one averaged structure should be observed. The transition state energy for rotation of one ${}^2A_{1g}$ structure into the next one is found to be at least 1.0 kcal mol⁻¹, in disagreement with the experimental value of 0.25 kcal mol⁻¹. This discrepancy might be due to relativistic effects or a breakdown of the rovibrational separation.

The third minimum which is obtained upon removal of an electron from the second component of the $1e_g$ orbital is about 3–5 kcal mol⁻¹ higher in energy at all correlated *ab initio* levels of theory and cannot compete with the 2A_g or the ${}^2A_{1g}$ minimum.

Acknowledgements H.M.S. acknowledges Wesley D. Allen for helpful discussions. This research was supported by the US National Science Foundation, Grant CHE-9527468.

References

- Koopmans, T. *Physica* 1 (1933) 104.
- Rabalais, J. W. and Katrib, A. *Mol. Phys.* 27 (1974) 923.
- Jahn, H. A. and Teller, E. *Proc. R. Soc. A* 161 (1937) 220.
- Liehr, A. D. *J. Chem. Phys.* 67 (1963) 389.
- Lathan, W. A., Curtiss, L. A. and Pople, J. A. *Mol. Phys.* 22 (1971) 1081.
- Lathan, W. A., Hehre, W. J. and Pople, J. A. *J. Am. Chem. Soc.* 93 (1971) 808.
- Baker, A. D., Baker, C., Brundle, C. R. and Turner, D. W. *Int. J. Mass Spectrom. Ion Phys.* 1 (1968) 285.
- Narayan, B. *Mol. Phys.* 23 (1972) 281.
- Richartz, A., Buenker, R. J., Bruna, P. J. and Peyerimhoff, S. D. *Mol. Phys.* 33 (1977) 1345.
- Richartz, A., Buenker, R. J. and Peyerimhoff, S. D. *Chem. Phys.* 28 (1978) 305.
- In the following the shorthand notation ag(eg) is employed to label the ag orbital that is obtained from the eg state after Jahn–Teller distortion and ag(a_{1g}) is used to characterize the ag orbital that is obtained from the 3a_{1g} orbital.
- Toriyama, K., Nunome, K. and Iwasaki, M. *J. Phys. Chem.* 85 (1981) 2149.
- Iwasaki, M., Toriyama, K. and Nuome, K. *J. Am. Chem. Soc.* 103 (1981) 3592.
- Toriyama, K., Nunome, K. and Iwasaki, M. *J. Chem. Phys.* 77 (1982) 5891.
- Iwasaki, M., Toriyama, K. and Nunome, K. *Chem. Phys. Lett.* 111 (1984) 309.
- Lunell, S. and Huang, M.-B. *J. Chem. Soc., Chem. Commun.* (1989) 1031.
- Huang, M.-B. and Lunell, S. *Chem. Phys.* 147 (1990) 85.
- Lunell, S., Eriksson, L. A. and Huang, M.-B. *J. Mol. Struct. (Theochem)* 230 (1991) 263.

19. Eriksson, L. A., Malkin, V. G., Malkina, O. L. and Salahub, D. R. *J. Chem. Phys.* 99 (1993) 9756.
20. The T_1 amplitudes for all the structures investigated in this study are smaller than 0.02. Hence they are very well described by a single reference and a multiconfigurational treatment is not necessary
21. Eriksson, L. A. and Lunell, S. *J. Phys. Chem.* 97 (1993) 12215.
22. GAUSSIAN 94, Revision C.3. Frisch, M. J., Trucks, G. W., Schlegel, H. B., Gill, P. M. W., Johnson, B. G., Robb, M. A., Cheeseman, J. R., Keith, T., Petersson, G. A., Montgomery, J. A., Raghavachari, K., Al-Laham, M. A., Zakrzewski, V. G., Ortiz, J. V., Foresman, J. B., Cioslowski, J., Stefanov, B. B., Nanayakkara, A., Challacombe, M., Peng, C. Y., Ayala, P. Y., Chen, W., Wong, M. W., Andres, J. L., Replogle, E. S., Gomperts, R., Martin, R. L., Fox, D. J., Binkley, J. S., Defrees, D. J., Baker, J., Stewart, J. P., Head-Gordon, M., Gonzalez, C. and Pople, J. A. Gaussian, Inc., Pittsburgh PA 1994.
23. Becke, A. D. *Phys. Rev. A* 38 (1988) 3098.
24. Miehlich, B., Savin, A., Stoll, H. and Preuss, H. *Chem. Phys. Lett.* 157 (1989) 200.
25. Lee, C., Yang, W., Parr, R. G. *Phys. Rev. B* 37 (1988) 785.
26. Becke, A. D. *J. Chem. Phys.* 98 (1993) 5648.
27. Becke, A. D. *J. Chem. Phys.* 98 (1992) 1372.
28. Stanton, J. F., Gauss, J., Watts, J. D., Lauderdale, W. J. and Bartlett, R. J. *Int. J. Quantum Chem.* S26 (1992) 879.
29. Davidson, E. R. and Borden, W. T. *J. Phys. Chem.* 87 (1983) 4783.
30. Brueckner, K. A. *Phys. Rev.* 96 (1954) 508.
31. Nesbet, R. K. *Phys. Rev.* 109 (1958) 1632.
32. Chiles, R. A. and Dykstra, C. E. *J. Chem. Phys.* 74 (1981) 4544.
33. Handy, N. C., Pople, J. A., Head-Gordon, M., Raghavachari, K. and Trucks, G. W. *Chem. Phys. Lett.* 164 (1989) 185.
34. Stanton, J. F., Gauss, J. and Bartlett, R. J. *J. Chem. Phys.* 97 (1992) 5554.
35. Huzinaga, S. *J. Chem. Phys.* 45 (1965) 1293.
36. Dunning, T. H. *J. Chem. Phys.* 53 (1970) 2823.
37. For the DFT and MP2 calculations five spherical d functions were employed.
38. Dunning, T. H. *J. Chem. Phys.* 55 (1971) 716.
39. PSI 2.0.8, Janssen, C. J., Seidl, E. T., Scuseria, G. E., Hamilton, T. P., Yamaguchi, Y., Remington, R. B., Xie, Y., Vacek, G., Sherrill, C. D., Crawford, T. D., Fermann, J. T., Allen, W. D., Brooks, B. R., Fitzgerald, G. B., Fox, D. J., Gaw, J. F., Handy, N. C., Laidig, W. D., Lee, T. J., Pitzer, R. M., Rice, J. E., Saxe, P., Scheiner, A. C. and Schaefer, H. F. Psitech, Inc., Watkinville 1994.
40. Bellville, D. J. and Bauld, N. L. *J. Am. Chem. Soc.* 104 (1982) 5700.
41. Eriksson, L. A., Lunell, S. and Boyd, R. J. *J. Am. Chem. Soc.* 115 (1993) 6896.
42. A much more detailed comparison between $C_2H_6^+$ and diborane can be found in Ref. 9.
43. Schreiner, P. R., Kim, S.-J., Schaefer, H. F. and Schleyer, P. v. R. *J. Chem. Phys.* 99 (1993) 3716.

Received June 27, 1996.